J Mater Sci: Mater Med (2010) 21:1211–1223
DOI 10.1007/s10856-009-3968-x

Nanostructured chitosan–surfactant matrices as polyphenols nanocapsules template with zero order release kinetics

Ana Gârlea · V. Melnig · M. I. Popa

Received: 22 April 2009 / Accepted: 6 December 2009 / Published online: 23 December 2009

Abstract Nanostructured membranes and films of cationic surfactant–chitosan with tannic acid as polyphenol model were obtained by phase inversion method. The membranes were investigated by Attenuated Total Reflectance Fourier Transform InfraRred, X-Ray Diffraction, Scanning Electron Microscopy and Thermogravimetry, and the films topography was analysed by Atomic Force Microscopy. The analysis reveals that the interactions at the molecular level between cationic CTAB surfactant and cationic chitosan polymer strive to weaken membrane stability, whereas, the tannic acid is favoured to cluster with CTAB and diminish the membrane thermodynamic instability. The nanocapsules formed, with dimensions in the range of 16.35–27.68 nm, are congregating in clusters having dimensions in the domain of 50–300 nm. The layers resulted from these nanostructures arrangement constitute a surfactant–chitosan matrix with tannic acid suitable for drug controlled release with zero order kinetics.

1 Introduction

The new tendency to design drug delivery systems consider the obtaining of pharmaceutical products with a good biodegradable and biocompatible profile, a good efficacy/toxicity ratio and adequate biopharmaceutical/pharmacokinetic characteristics.

While the synthetic polymers are used as matrix for their advantageous synthesis design properties and wide choice availability, the natural polymers have been used for their high biocompatibility and less immunogenicity.

The problem of polymer matrix design is considered also from the point of view of the bioavailability of drugs. It was demonstrated that opsonization, recognition and phagocytosis by macrophages are strongly dependent on the mucoadhesive polymer matrix properties and the dimension of the active principle particles [1, 2]. It was found that particles with a diameter smaller than 200 nm manifest a decreased rate of clearance and thus an extended circulation time as compared to those with a larger diameter [2, 3]. As a result, there are increased interests to clarify the terminology in correlation with the major features of each type and the methods used for nanoparticulate structures obtaining, the factors that influence the formation of particular nanoparticulate formulations (nanocontainers, micelles, nanospheres, nanocapsules and polymersomes) and to examine the factors that influence the physicochemical properties of the formed system.

In particular, chitosan seems to be an appropriate candidate for nanoparticulate systems design. Oral delivery of salmon calcitonin has recently been used as nanocapsules composed of a copolymer of polyethylene glycol and chitosan [4].

In the first instance, chitosan appears economically attractive since it can be obtained from deacetylation of chitin, the second most abundant biopolymer in nature next to cellulose. Chitosans present varied physicochemical properties related to the molecular weight, the elongation at break, the tensile strength and, also, biological properties, including the biodegradation by lysozyme and the wound-healing properties [5].

A. Gârlea · V. Melnig (✉)
Characterization of Molecular Organization in BioMaterials Laboratory, Department of Physics, Faculty of Physics, "Alexandru Ioan Cuza din Iasi" University, 11A, Carol I Blvd., Iasi 700506, Romania
e-mail: vmelnig@uaic.ro

M. I. Popa
Faculty of Chemical Engineering and Environment Protection, "Gh. Asachi" Technical University, 71 A, D. Mangeron St., 700050 Iasi, Romania

Due to its high content of primary amines, chitosan physically interacts with different ionic surfactants allowing to be functionalised or to cross-link its backbone, thus improving the chitosan mechanical properties.

Chitosan was chosen as matrix for the polyphenol entrapment because of the unusual combination of its properties, namely an excellent ability of membrane forming, high water permeability, high mechanical strength, good adhesion and biocompatibility [6].

Recently, some coworkers obtained chitosan/alginate/tannic acid microparticles by co-precipitation method [7]. The interest for using tannic acid in drug delivery systems derives from tannic acid (TA) properties and abundance in the bark and fruits of many plants. This hydrolysable polyphenol has a structure consisting of a central carbohydrate (glucose) and 10 galloyl groups [8, 9].

Several authors have demonstrated that tannic acid and other polyphenols have antimutagenic and anticarcinogenic activities [9–14]. The consumption of fruits, vegetables, and beverages, such as tea and red wine, which contains polyphenols, has been associated with the inhibitory and preventive effect in multiple human cancers and cardiovascular diseases [9, 11, 13–19], which may be correlated (at least in part) with the antioxidant activity of polyphenols [14–17].

As was highlighted in [7] this active principle should not be used in high quantities because inhibits the absorption of iron in the body and the effectiveness of digestive enzymes [20].

In a previous study [21], we have prepared by dry phase inversion freestanding cross-linked chitosan films from solutions of chitosan in acetic acid, in the presence of a moderate amount of cationic and anionic surfactant, namely Cetyltrimethylammonium bromide (CTAB) and Sodium dodecyl sulfate (SDS), respectively. The results revealed that the films obtained have a high degree of order at nanoscale level by formation of surfactant nanocrystals networks, due to the hydrophilic/hydrophobic balance interactions. These networks can be candidates as drug nanocapsules host by associative trapping phenomena.

The aim of this study is the side effects removal by making controlled drug delivery systems with zero order kinetics, for *per os* administration, of TA–cationic surfactant nanocapsules in chitosan-based matrix.

2 Experimental

2.1 Materials

The chitosan was provided by Vanson Chemicals Redmond WA, USA. The N-deacetylation degree was 79.7%, the average molecular weight was $M_w = 310{,}000$ g/mol and the polydispersity index was 3.26. All chemicals are reagent grade: tannic acid, $M_w = 1701.20$ g/mol, purchased from Sigma–Aldrich; CTAB, from Chemapol; SDS from Sigma; acetic acid 99.5% and ethyl alcohol 94%, from Chemical Company; RBS 35 concentrate solution from Fluka.

2.2 Sample preparation

A. Freestanding cross-linked chitosan films from solutions of chitosan in acetic acid, in the presence of a moderate amount of CTAB and SDS, were prepared in the first stage. The preparation protocol sketch, of precursor chitosan based nanofilms and thick membranes containing CTAB or SDS surfactants, is presented in Fig. 1. Respecting the same protocol, chitosan based nanofilms and thick membranes containing different amounts of tannic acid were prepared to be used as blank tests.

Chitosan solutions (2 and 3% biopolymer concentration in 1% acetic acid) with different surfactant concentrations (2, 4, 6, 8 and 10 m*m*) were prepared. The mixtures were stirred at room temperature for 24 h, and the solutions were centrifuged at 4000 rpm/30 min for degassing.

For the preparation of the investigated chitosan membranes the dry phase inversion method was used: initially, the solutions were poured into Teflon moulds and left for evaporation in a thermostat chamber at 50°C for 24 h.

The nanofilms were obtained by depositing on 25 × 25 mm^2 area clean microscope glass slides by spin-coating method using a WS-400B-6NPP/LITE spin-coater.

The microscope glass supports were cleaned with a dish detergent, followed by a thorough rinsing with deionised water and ethyl alcohol. After that, the microscope glass supports were sonicated (Sonoplus, Bandelin, 20 kHz, at 15 W) for 10 min while submerged in a 2% RBS 35 concentrate solution, followed by a second rinse with ethanol and deionised water. The summary of the prepared samples is presented in Table 1.

As is motivated in Sect. 4.1, the precursor solutions of the chitosan (2 or 3%)–CTAB (6 m*m*) membranes, are suitable to favor the clustering and shelling nanoscale process of tannic acid with CTAB.

B. Two matrices of 2 and 3% chitosan solutions were prepared in a similar way as in subsection **A**, by mixing the 6 m*m* cationic surfactant (CTAB) with different concentrations of tannic acid (1, 3, 5, 7 and 10 m*m*). The preparation protocol sketch is similar with the one from Fig. 1 and the summary of the prepared samples is presented in Table 2.

3 Results

3.1 Characterization analyses

The Attenuated Total Reflectance Fourier Transform InfraRred (ATR-FTIR) spectra were taken with a BOMEM

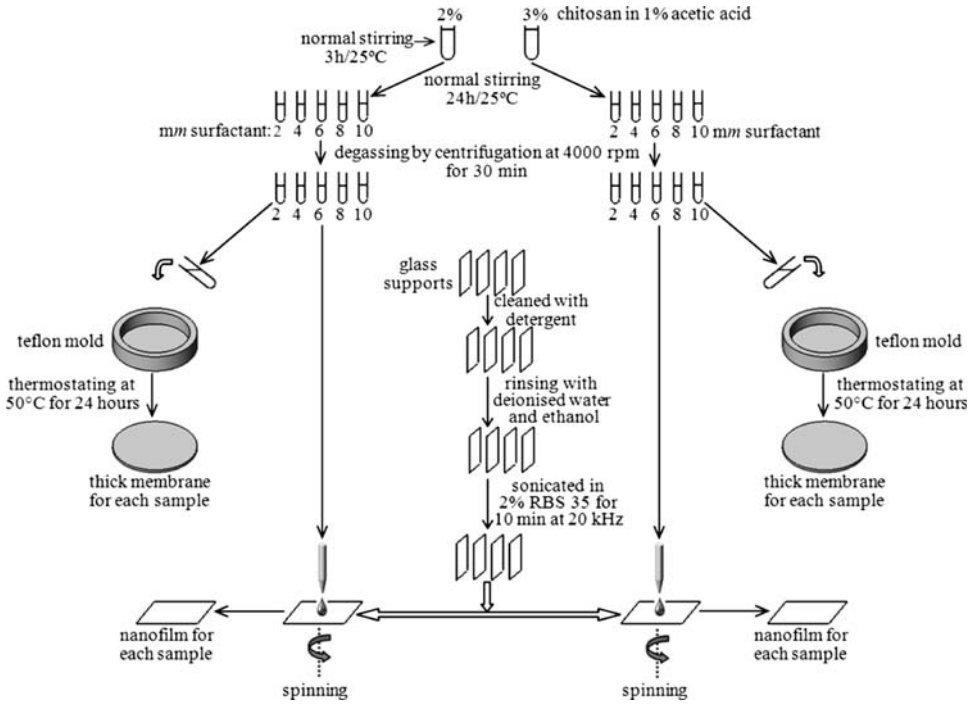

Fig. 1 Chitosan based nanofilms and thick membranes, containing CTAB and SDS surfactants, preparation protocol sketch

Table 1 Summary of the prepared samples of chitosan based nanofilms and thick membranes, containing CTAB and SDS surfactants

Sample code	Type	Concentration		
		Chitosan (%)	CTAB	SDS
M2CH	Membrane	2	–	–
F2CH	Film			
M2CHXC	Membrane	2	X = 2; 4; 6; 8; 10 m*m*	–
F2CHXC	Film			
M2CHXS	Membrane	2	–	X = 2; 4; 6; 8; 10 m*m*
F2CHXS	Film			
M3CHXC	Membrane	3	X = 2; 4; 6; 8; 10 m*m*	–
F3CHXC	Film			
M3CHXS	Membrane	3	–	X = 2; 4; 6; 8; 10 m*m*
F3CHXS	Film			

MB-104 spectrometer, with a 4 cm^{-1} resolution in the range of 4000–500 cm^{-1}.

The microphase structure was investigated by X-Ray diffraction (XRD), performed on a DRON-2 diffractometer, employing nickel-filtered Cu K_α radiation (1.54182 Å) at 25 kV operational voltage.

Table 2 Summary of the prepared samples of 2 and 3% chitosan based nanofilms and thick membranes, containing 6 m*m* CTAB with different concentrations of tannic acid (1, 3, 5, 7 and 10 m*m*)

Sample code	Type	Concentration	
		Chitosan (%)	Tannic acid
M2CH6CYTA	Membrane	2	Y = 1; 3; 5; 7; 10 m*m*
F2CH6CYTA	Film		
M3CH6CYTA	Membrane	3	Y = 1; 3; 5; 7; 10 m*m*
F3CH6CYTA	Film		

The order degree was evaluated by computing the interplanar distances, D, using the Bragg relation:

$$2D \sin \theta = n\lambda \quad (1)$$

where n is an integer determined by the order given, θ is the angle between the incident ray and the scattering planes, λ is the wavelength of X-ray and D is the spacing between the planes in the atomic lattice of sample (the interplanar distance).

The crystallites size was determined from X-ray diffractograms according to Scherrer relationship [22]:

$$L = \frac{K\lambda}{\beta \cos \theta} \quad (2)$$

where L is the diameter (thickness) of crystallite, K is a constant dependent on crystallite shape (0.89) and β is the full line width at half max.

The films topographies were analyzed by Atomic Force Microscopy (AFM) using a Solver Pro 7 M apparatus. The analysis was made in tapping mode.

The morphology of membranes was studied by Scanning Electron Microscopy (SEM) on a VEGA TESCAN apparatus.

Thermogravimetric analysis (TGA) was performed under nitrogen flow (20 mL/min) at a 10°C/min heating rate from 25 to 900°C with a Mettler Toledo model TGA/SDTA 851e. The initial mass of the samples was between 2 and 5 mg. For a good evaluation of the percentage mass loss, $W\%$, and the residue, the T_{endset} of the final stage of membranes thermograms was extrapolated to 900°C.

The drug release kinetic studies were made using a NanoDrop-1000 spectrophotometer, for which the sample quantity required is of microlitres order. This device is very convenient for this kind of studies because the analysis time is extremely short and the used quantities are small, so that the process and the eluent concentration can be considered unchanged.

The drug release kinetic studies from membranes were performed in three liquid models having different pH values: hydrochloric acid (pH = 2.0—gastric liquid), phosphate buffer solution (pH = 5.2—moderate pH) and urea (pH = 9.3—intestinal medium).

The drug release kinetic studies were made by submerging 20 mg of membrane in 50 mL eluent, taking samples at different times and measuring the drug absorbance. The samples were kept at the constant temperature of 37°C. The measurements were carried out in the UV range, at the wavelength of 277 nm where the tannic acid spectrum presents a maximum. At this wavelength, neither the solvent nor the polymer absorbs UV light.

To calculate the concentration of the released drug from the samples it was drawn the calibration curve in water for tannic acid (the calibration curves in phosphate buffer solution and hydrochloric acid do not differ from that in water). For this purpose, it was introduced 0.02 g of each sample in 50 mL of 0.5 N hydrochloric acid and maintained in this solution for 30 h, during which the release is total. The absorbance of each solution has been measured and based on the calibration curve, the concentration, respective the drug quantity, was calculated. The equation and the mean square deviation (R^2) for this curve are: $A = 0.043 \times c, R^2 = 0.999$.

3.2 CTAB and SDS chitosan based nanofilms and thick membranes analysis

The AFM images of F2CH, F2CH6C and F2CH2TA as blank tests are presented in Fig. 2.

The SEM micrographs for chitosan membranes with a 2% concentration, in the presence of different CTAB amounts are shown in Fig. 3. Similar SEM micrographs were obtained for 3% chitosan membranes with different CTAB amounts.

The corresponding X-ray diffractograms of chitosan membranes with 2 and 3% concentration, in the presence of CTAB are presented in Fig. 4.

The FTIR spectra for M2CH, M2CH2C, M2CH6C and M2CH10C are shown in Fig. 5; no major differences are obtained in the case of 3% chitosan membranes with CTAB.

3.3 Chitosan based nanofilms and thick membranes containing tannic acid in the presence of CTAB analysis

The AFM images of 2% chitosan based films with 6 m*m* CTAB and different concentration of tannic acid are presented in Fig. 6. Similar results were obtained for 3% chitosan membranes with 6 m*m* CTAB and different concentration of tannic acid.

The FTIR spectra of M2CH6C3TA, M2CH6C7TA and M2CH6C10TA are shown in Fig. 7; no major differences are obtained in the case of 3% chitosan membranes.

The corresponding X-ray diffractograms of 2% and 3% chitosan concentration membranes with 6 m*m* CTAB and 3, 7, 10 m*m* tannic acid are presented in Fig. 8.

The SEM images of M2CH6C3TA, M2CH6C7TA and M2CH6C10TA are presented in Fig. 9; similar micrographs were obtained for matrices containing 3% chitosan.

The thermogravimetry (TG) and differential thermogravimetry (DTG) curves recorded for M2CH6C and M2CH6C7TA representative samples membranes are shown in Fig. 10.

The drug release curves of the 2 and 3% chitosan matrices with 6 m*m* CTAB and relevant tannic acid concentrations are shown in Figs. 11, 12, 13.

4 Discussions

4.1 CTAB and SDS chitosan based nanofilms and thick membranes

In the absence of a cross-linker molecule the chitosan membranes obtained are semitransparent, quite hard and breakable. Also, a large drying time before gellating step determines a dense membrane formation in which the internal tensions increase with the membrane thickness [5, 23]. In the case of surfactant addition, the tensions become locally distributed and this determines a high degree of order at the nanoscale level. The surface energy analysis

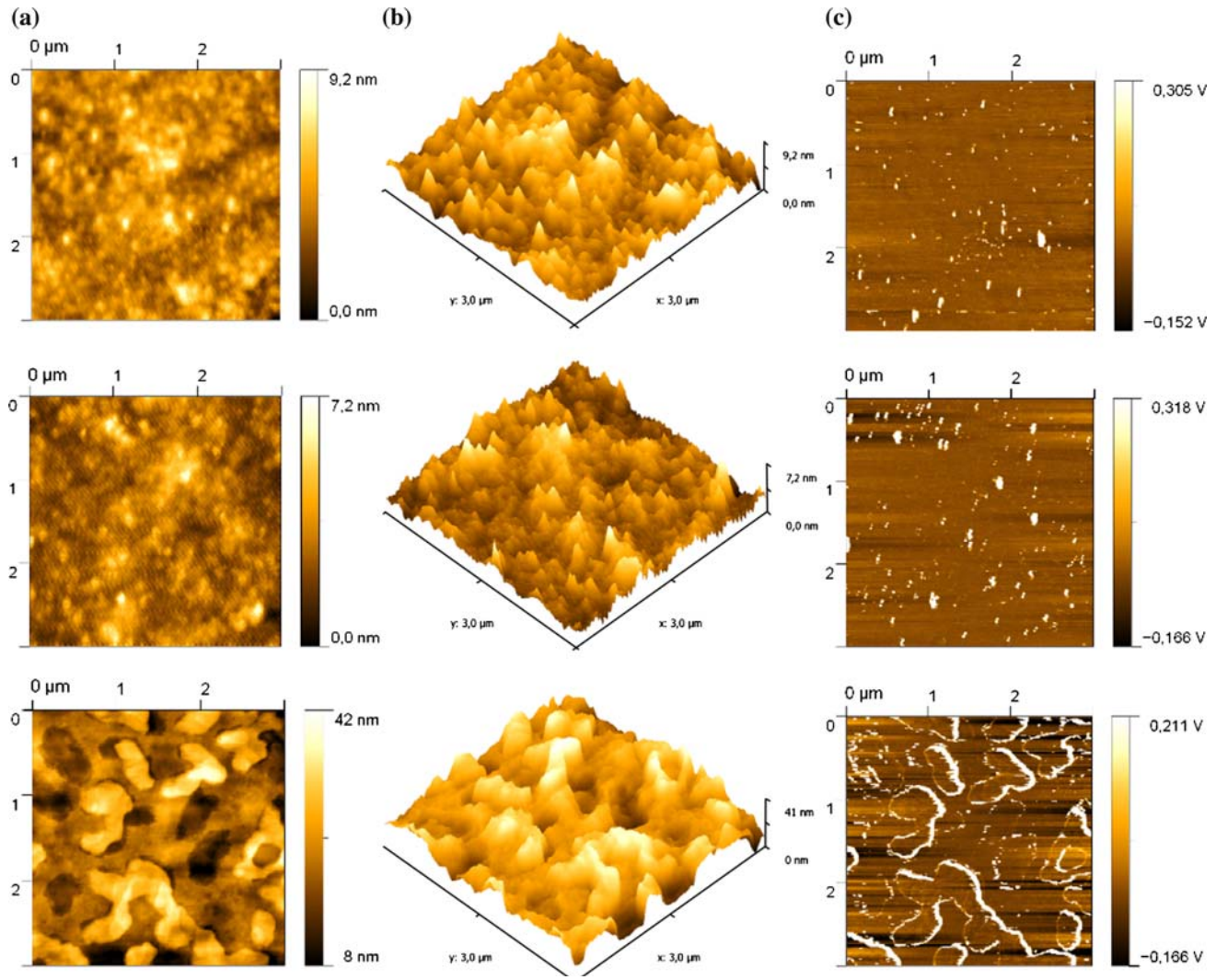

Fig. 2 2D (**a**) and 3D (**b**) topographies, and phase contrast (**c**) of F2CH (*top*), F2CH2TA (*middle*) and F2CH6C (*bottom*); the scale of square area is 3 × 3 μm^2

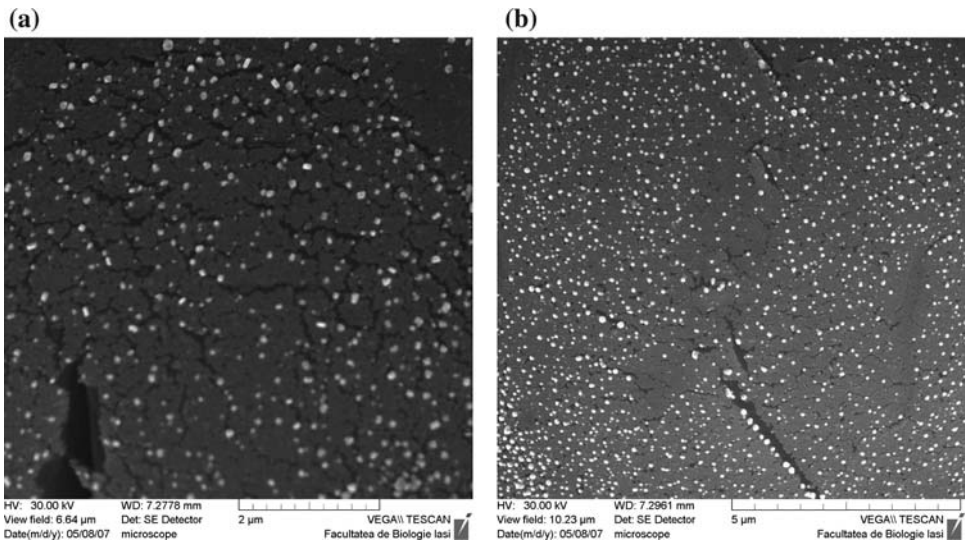

Fig. 3 SEM micrographs of air-facing surfaces for M2CH6C (**a**) and M2CH10C (**b**)

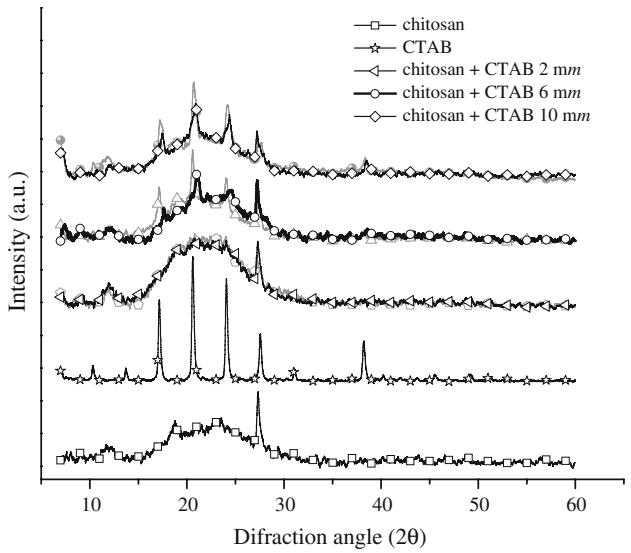

Fig. 4 X-Ray diagrams for chitosan membranes with 2% (*grey*) and 3% (*black*) concentration, in the presence of CTAB

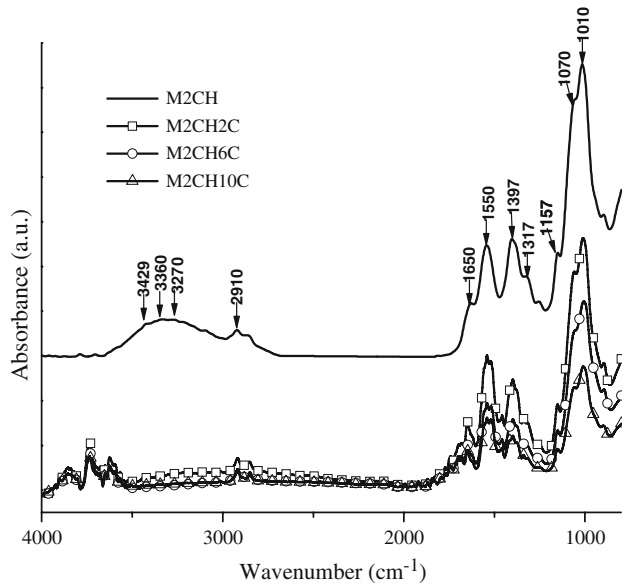

Fig. 5 FTIR spectra for 2% pure chitosan membrane and chitosan membranes in the presence of different concentrations of CTAB

revealed that the CTAB–chitosan membranes are more hydrophilic than the SDS–chitosan membranes [21]. Although the chitosan–SDS membranes, being more hydrophobic, are better aspirants for controlled drug release matrices, only those with chitosan and CTAB were chosen due to the low toxicity of CTAB surfactant compared with SDS [24, 25].

4.1.1 Nanophase materials analysis

For a better understanding of the molecular assembling processes, AFM topographies of different combinations of film constituents were performed (Fig. 2). It can be observed that the chitosan and tannic acid–chitosan system films are homogeneous while the CTAB–chitosan system film have a heterogeneous morphology (the two, chitosan and CTAB, have cationic behavior) with a good regularity at the nanophasic level.

As can be seen from SEM picture (Fig. 3) and from X-Ray diffractograms (Fig. 4), the membranes are dense and have a uniform nanocrystals distribution.

4.1.2 Structural analysis

The X-ray diffractogram of pure chitosan shows an almost amorphous structure while, as expected, the membranes with CTAB show an apparent increase in crystallinity with the increase of CTAB concentration. The fact that the intensity of diffraction peaks increases with the increase of CTAB concentration, without any modification of the position of those peaks, shows that these diffractograms are the result of interference patterns composition from the two structures, the chitosan matrix and CTAB clusters.

To evaluate the ordering degree and nanometric domains dimension, the interplanar distances, D, were calculated using Bragg relation (1) and the nanodomains dimensions, L, using Scherrer relation (2). The obtained results are synthetically presented in Table 3.

From this table it can be concluded that chitosan presents a certain crystallinity degree, known from literature, the most intense maximum being at $2\theta = 27.25$, for which $D = 0.32$ nm and the nanometric domains have a dimension of $L = 17.96$ nm.

In the presence of CTAB surfactant, membranes with a high crystallinity degree and a complex interplanar structure are obtained, having a nanometric domains distribution of dimensions that ranged within 60–180 nm (determined from SEM micrographs) and within 8.38–20.36 nm (from X-ray diffractograms), respectively.

Comparing these values with those of pure CTAB nanocrystals and with those of chitosan it can be concluded that surfactant in association with chitosan dictates a certain ordering degree of the domains which determines the complex nano- meso-phasic structure.

Chitosan FTIR spectrum from Fig. 5 exhibits characteristic absorption bands of amide I at 1650 cm^{-1} (C=O stretching), amide II at 1550 cm^{-1} (N–H in plane deformation coupled with C–N stretching), amide III (C–N stretching coupled with NH in plane deformation) and CH_2 wagging coupled with OH in plane deformation at 1317 cm^{-1}. In the functional group region, the broad peak observed at 3450–3200 cm^{-1} is the result of the different specific vibrations: the hydrogen-bonded OH stretching at 3429 cm^{-1}, the NH_2 asymmetric stretching at 3360 cm^{-1}

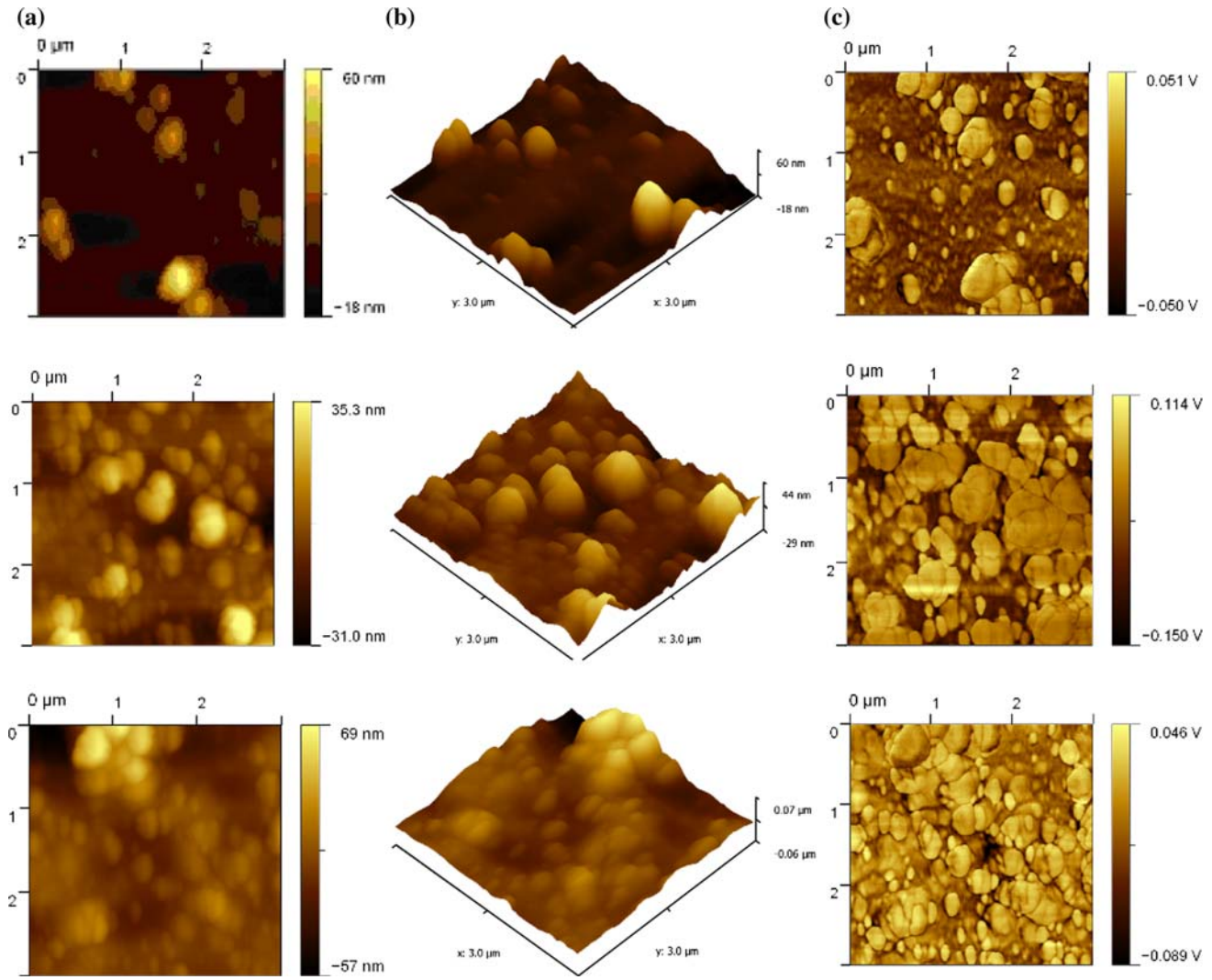

Fig. 6 2D (**a**) and 3D (**b**) topographies, and phase contrast (**c**) of F2CH6C3TA (*top*), F2CH6C7TA (*middle*) and F2CH6C10TA (*bottom*); the scale of square area is 3 × 3 µm^2

and the NH stretching in interchain NH···O=C bonding at 3270 cm^{-1}.

The other peaks at 2910 and 1397 cm^{-1} were assigned to CH stretching and CH_3 symmetric deformation, respectively. Anti-symmetric stretching of C–O–C gives a narrow band at 1157 cm^{-1}. The skeletal vibrations involving the C–O stretching at 1070 and 1020 cm^{-1} are characteristics bands of the chitosan saccharide structure [5, 26, 27]. The absence of the sharp absorption peak around 3500 cm^{-1} indicates that there are no free OH groups.

Comparing the spectrum of 2% pure chitosan membrane with those of chitosan membranes with CTAB, from Fig. 5, despite the fact that both molecules (chitosan and CTAB) present cationic character, it can be observed that interactions occur, and this is evidenced by the modification of the groups absorption bands. While in the fingerprint region the absorption bands intensities are proportional attenuated with the CTAB concentration increasing, in respect of position and profile of absorption bands, the functional group region is drastically affected by the presence of CTAB at whatever concentration; peaks being observed beyond 3500 cm^{-1}.

The bands within 3500–3000 cm^{-1} shifted to high frequencies indicate an increase in the ordered structure [28]. The region 1500–1200 cm^{-1} is related to the local symmetry.

Resuming, the fact that chitosan membranes are flexible when the surfactant is added (based on the results obtained from FTIR, XRD and AFM analysis) entitle us to affirm that the internal tensions, arising from chitosan membrane solidification, become locally distributed at the interface with CTAB nanometer domains. It is possible that the repulsion interactions occurring between the two types of molecules (chitosan and CTAB), due to their cationic

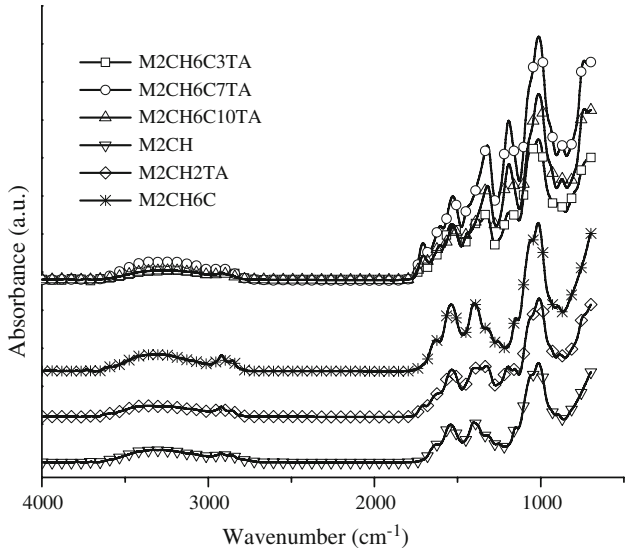

Fig. 7 FTIR spectra of 2% chitosan and 6 m*m* CTAB membranes in combination with different tannic acid concentrations

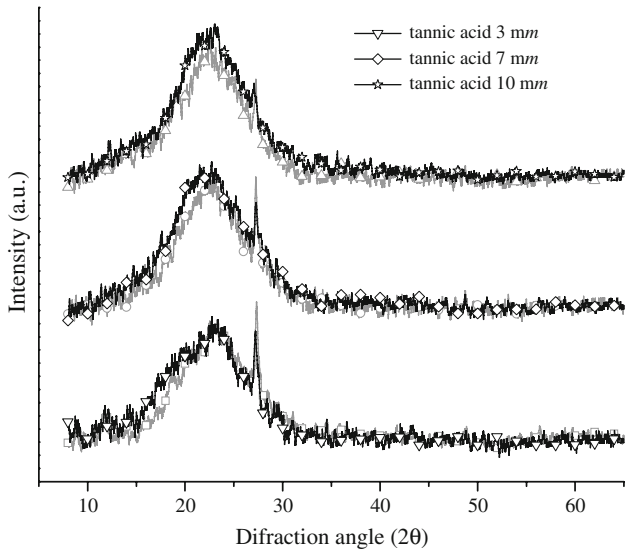

Fig. 8 X-Ray diagrams for 2% (*grey*) and 3% (*black*) chitosan membranes with CTAB 6 m*m* and different concentration of tannic acid

behaviour in aqueous solution, to reduce the internal tensions. In addition, the solidification process of the membrane, held at constant temperature, is completed with a mixture of two solid phases in equilibrium (there is no phase separation). Thus, we can consider that the system in liquid phase passes through several quasiequilibrium states until an appreciable amount of solvent (water) is lost and the system becomes a solid membrane. It is important to discuss at least two antagonistic processes competing to achieve system stability: the migration process due to mutual repulsions between the two types of cationic molecules and the process due to CTAB molecules diffusion. The measure of kinetic forces associated with the above mentioned processes highly determines the nanocapsules size and their uniform distribution in the horizontal planes. From the structural point of view, FTIR analysis shows that there are interactions between the two types of molecules. Any disturbance of a molecule from the in vacuum state alters the symmetry of the isolated molecule. The interactions between these two types of molecules lead to a local order at nanometer level of CTAB domains, in detriment to molecular symmetry, without a major influence on crystalline degree of chitosan matrix.

The analysis from this section reveals that the optimum concentrations, for ordering degree, were obtained for 2–3% chitosan and CTAB concentration in the range 6–10 m*m*. Practically, a minimum concentration of 6 m*m* CTAB was chosen to minimize the effects due to this surfactant, although it is considered as having a low toxicity [24, 25].

4.2 Chitosan based nanofilms and thick membranes containing tannic acid in the presence of CTAB

4.2.1 Nanophase materials analysis by AFM

From the AFM images (Fig. 6) it can be observed that there is a tendency for the tannic acid–CTAB nanocapsules to agglomerate in clusters both in the case of 2 and 3% chitosan based films. Also, the net structures of those types that can be seen from the bottom of Fig. 1 for CTAB do not appear and the fact that these structures have a geometrical form approximately of the same type and increase in ponderosity with the increase of the tannic acid concentration, entitle us to believe that they contain a tannic acid–CTAB mixture (they are capsules). These clusters are well defined by the chitosan matrix and for that reason we suppose that they will have different solubility behavior unlike the chitosan matrices.

4.2.2 Structural analysis

The wide range of nanoclusters dimensions hide/destroy the mesophasic ordering, in spite of the regularity in the horizontal plane. These are reflected in ATR–FTIR spectra (Fig. 7) and X-ray diffractograms (Fig. 8). The absorbance and the areas of the peaks in the 1500–1700 cm^{-1} region decreased in the presence of tannic acid, while the skeletal vibrations involving the C–O stretching at 1070 and 1020 cm^{-1} are not major affected.

The local symmetry is drastically changed by the modifications produced in the peaks ponderosity within the

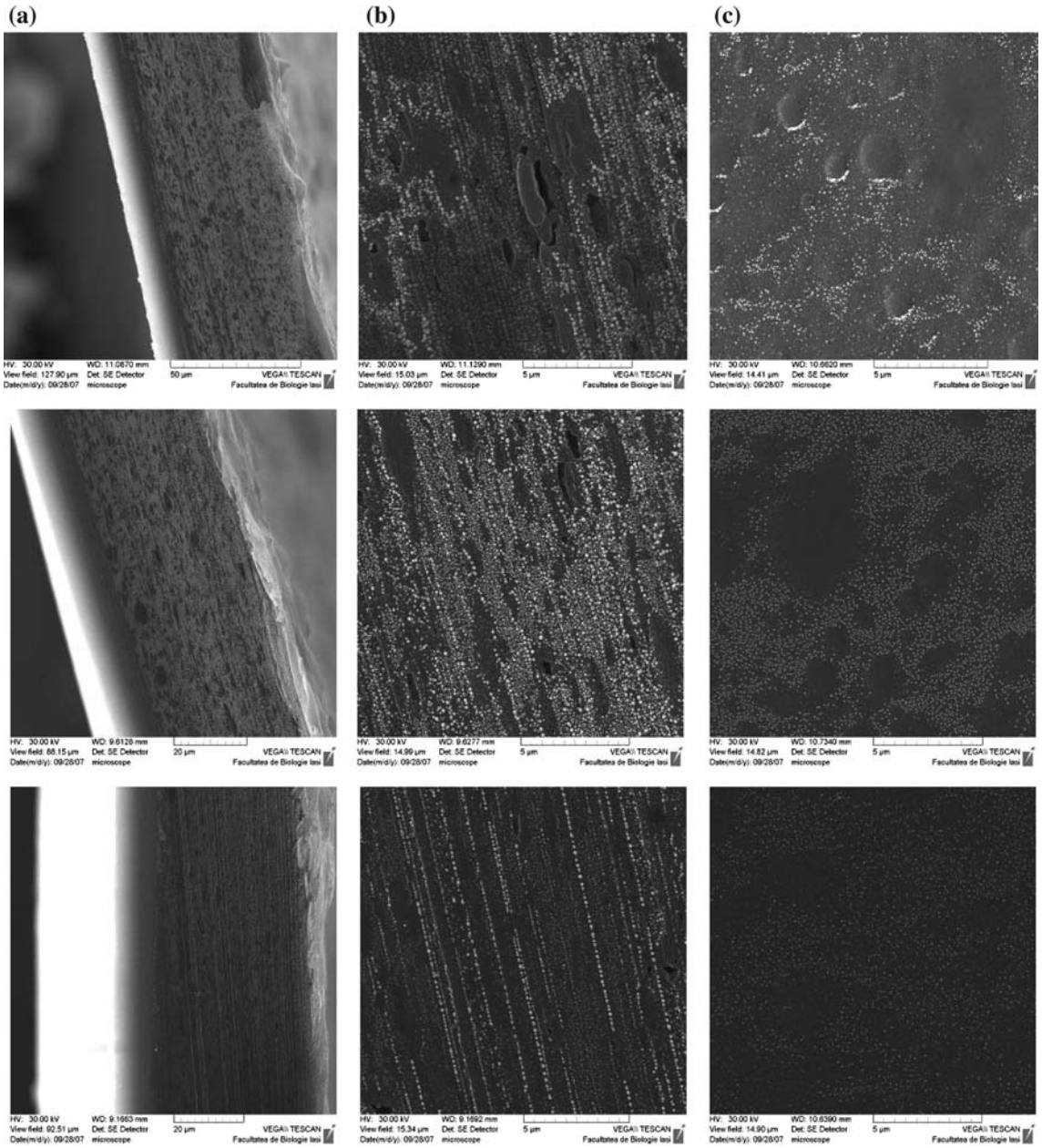

Fig. 9 SEM micrographs of transversal section (**a**), transversal section details (**b**) and air-facing surface (**c**) of M2CH6C3TA (*top*), M2CH6C7TA (*middle*) and M2CH6C10TA (*bottom*)

1500–1200 cm^{-1} region. The functional group region is drastically affected by the presence of tannic acid, whatever the concentration, with no shifting to high frequencies.

The X-ray diffractograms reveal a crystallinity increasing with the tannic acid concentration increase and a mesophasic ordering decreasing due to the wide range of cluster dimensions. The nanodomains dimensions, *L*, computed by Scherrer relation (2) are 3–5 times bigger than in the case of CTAB clusters varying from 16.35 to 27.68 nm, while interplanar distances, *D*, are not sensible diminished (Table 4).

4.2.3 Nanophase materials analysis by SEM

From the SEM images (Fig. 9) it can be observed that the membranes are dense, homogenous, without pore structures, except for a few accidental craters that do not have any spatial regularity.

The SEM images demonstrate an ordering of the tannic acid–CTAB capsules in horizontal planes, which means that these nanocapsules will controlled release the active substance (tannic acid, in this case) as the chitosan matrix is subject of the swelling–erosion process.

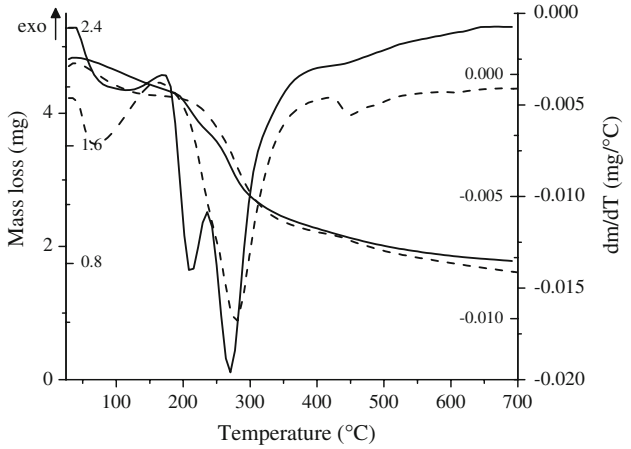

Fig. 10 TG and DTG curve for M2CH6C (*dash line*; vertical scales inside) and M2CH6C7TA (*solid line*; vertical scales outside) membranes

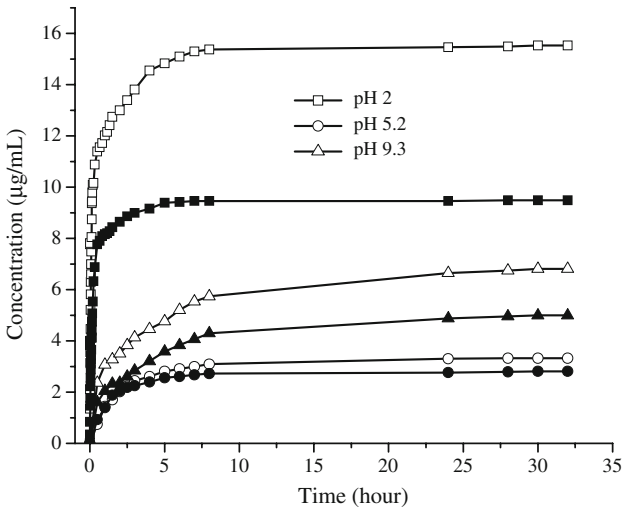

Fig. 12 Kinetic curves for tannic acid release from M2CH6C7TA (*open symbols*) and M3CH6C7TA (*filled symbols*)

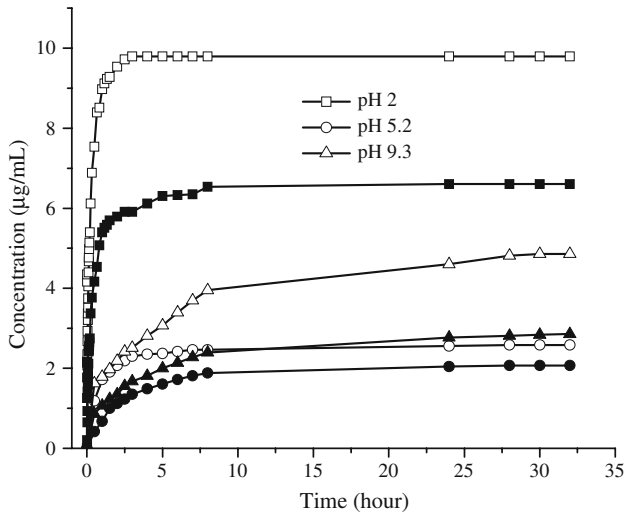

Fig. 11 Kinetic curves for tannic acid release from M2CH6C5TA (*open symbols*) and M3CH6C5TA (*filled symbols*)

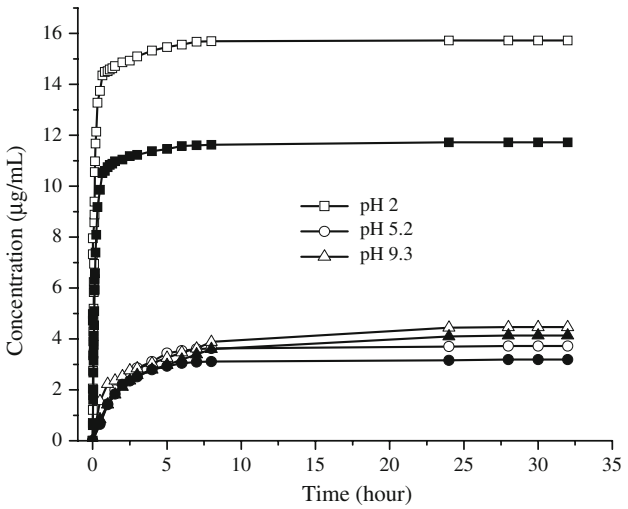

Fig. 13 Kinetic curves for tannic acid release from M2CH6C10TA (**a**) and M3CH6C10TA (**b**)

The air-facing surface SEM images indicate that at low tannic acid concentration the nanocapsules are distributed as islands and with the concentration increase, these planes become better distributed.

Moreover, it seems that with the increase of tannic acid concentration there is a tendency of the capsules to homogenize (dissolute) in chitosan matrix. This is in good concordance with the AFM images from Fig. 1 of tannic acid–chitosan system films. This fact means that over a concentration of 10 m*m* tannic acid the capsules formation is diminished.

By visual analysis of the SEM micrographs it can be observed that the nanocapsules have dimensions in the range of 50–300 nm for tannic acid.

Table 3 Crystalline characteristics of surfactant–chitosan membranes obtained from the X-ray diffractograms (for the most intense maximum of chitosan)

Sample	$2\theta(^\circ)$	Intensity(a.u.)	D(nm)	L(nm)
Chitosan	27.25	56.77	0.32	17.96
CTAB	27.47	41.44	0.32	27.96
M2CH2C	27.15	41.09	0.21	–
M2CH6C	27.36	30.29	0.32	12.39
M2CH10C	27.42	56.10	0.32	8.38
M3CH2C	27.48	51.02	0.32	13.91
M3CH6C	27.37	53.51	0.32	20.36
M3CH10C	27.18	35.84	0.32	13.57

Table 4 Crystalline characteristics of chitosan with tannic acid-CTAB membranes obtained from the X-ray diffractograms (for the most intense maximum of chitosan)

Sample	$2\theta(^\circ)$	Intensity(a.u.)	D(nm)	L(nm)
M2CH6C3TA	27.33	29.93	0.32	26.96
M2CH6C7TA	27.26	32.83	0.32	24.88
M2CH6C10TA	27.26	22.62	0.32	26.99
M3CH6C3TA	27.22	26.56	0.32	21.17
M3CH6C7TA	27.29	17.97	0.32	27.68
M3CH6C10TA	27.08	12.43	0.32	16.35

4.2.4 Thermogravimetric structural analysis

The thermogravimetric characteristics of TG and DTG analysis from Fig. 10 are presented in Table 5.

Thermal degradation of membranes is best analyzed with reference to the corresponding chitosan films thermograms [5, 29, 30] that exhibits two distinct stages. The endothermal one, in the range of about 40–180°C peaking at 75°C, is associated with evaporation of the acetic acid and water solvent traces used for chitosan films preparation. The presence of two peaks, one at 110°C and the other at 160°C indicates that there are different degrees of association of water with the membrane components [5]. The other one, in the range of 224–418°C with maximum decomposition rate at 306°C, has been ascribed to a complex process including dehydration of the saccharide rings, depolymerization and decomposition of the acetylated and deacetylated units of the polymer. A possible decomposition thermo-oxidative process stage starts above 540°C up to 820°C [5].

In the range of interest (40–700°C) the presence of CTAB in chitosan membrane is viewed by the water amount enhancement (stage I) and by the decomposition stage (stage III) because of the weaken membrane stability due to the chitosan chain fragmentation by the CTAB surfactant and to the repulsions between these two cationic compounds.

Table 5 Thermogravimetric characteristics

Sample	Stage	T_{onset}	T_{peak}	T_{endset}	$W(\%)$	Residue(%)
M2CH6C	I	46.7	64.6	137.9	10.30	27.43
	II	228.2	278.9	310.4	42.95	
	III	439.8	446.5	463.0	19.32	
M2CH6C7TA	I	58.9	91.4	190.2	10.95	36.8
	II	195.1	209.9	228.0	15.36	
	III	255.5	269.9	282.0	36.89	
	IV	388.0	431.5	484.0		

T_{onset} temperature at which the degradation begins in each stage, T_{peak} temperature at which the degradation rate is maximum, T_{endset} temperature at which degradation is finished in each given stage, $W\%$ percentage mass loss and the *residue* ash that is left after heating the sample to 900°C

In the case of M2CH6C7TA, the DTG shows two-stage decomposition within 190–300°C in contrast to M2CH6C. The stage II corresponds to the melting process of tannic acid nanocrystals (tannic acid crystal melting point: $T_m = 210°C$). The stage III correspond to the stage II of pristine chitosan and chitosan–CTAB membranes—the complex processes of dehydration of the saccharide rings, depolymerization and decomposition of the acetylated and deacetylated units of the polymer.

The presence of tannic acid, as can be expected, enhances the water retention in membrane (stage I), but the destabilization membrane process owing to CTAB is diminished, the stage IV being practically irrelevant comparing the chitosan–CTAB stage III.

Corroborating the thermogravimetric analysis with data from AFM, SEM and FTIR one can conclude that there are interactions at the molecular level between cationic CTAB surfactant and cationic chitosan polymer that strive to weaken membrane stability whereas, respecting the local conditions of equilibrium, the tannic acid is favored to cluster with CTAB. This diminishes the membrane thermodynamic instability by engaging in interactions the CTAB functional groups. The result is a tannic acid nanoencapsulation in chitosan matrix.

4.2.5 The drug release kinetic studies

The precise quantities of membranes submerged in the three different eluents, where they were kept for 32 h, release the tannic acid in a different way. The membrane partial degradation in hydrochloric acid (pH = 2.0) took place in more than 32 h, while the membranes from the eluents with pH = 5.2 and pH = 9.3 remained practically nondegradated during this time. An erosion and diffusion complex process was observed, the diffusion process being faster in the acid medium than in the others.

It can be said that in hydrochloric acid (pH = 2.0), after a relatively short time, the kinetic is of zero order, while in pH 5.2 and 9.3 the kinetic becomes of zero order after approximately 7 h. We can affirm that this kind of nanostructured matrix is pH-sensitive being suitable for releasing both in stomach and intestine, the diurnal cycle allowing the required time for releasing.

The percentage of tannic acid released from M2CH6C10TA was: 90% in pH 2.0, 20% in pH 5.2 and 25% in pH 9.3. In the case of M3CH6C10TA the percentage released was: 90% in pH 2.0, 25% in pH 5.2 and 31% in pH 9.3. It can be observed that the tannic acid minimum amount release is produces in all cases at moderate pH. This is determined by the fact that the zero order kinetic is governed by the erosion and diffusion complex

process, being known that the erosion process is rate restrictive and is favored by the extreme pH.

5 Conclusions

Membranes with a high degree of order at nanoscale level were obtained by dry phase inversion preparation from solutions of chitosan in acetic acid, in the presence of a moderate amount of CTAB cationic surfactant.

The addition of tannic acid increases the crystallinity of membrane and decreases the mesophasic order due to the wide range of cluster dimensions.

From the corroboration of the TG, DTG, AFM, SEM and FTIR analyses we conclude that, there are interactions at molecular level between cationic CTAB surfactant and cationic chitosan polymer that strive to weaken membrane stability. However, respecting the local conditions of equilibrium, the tannic acid is favored to cluster with CTAB and diminish the membrane thermodynamic instability by engaging in interactions the CTAB functional groups. The result is a chitosan matrix with nanocapsules.

By SEM micrographs it can be observed that the nanocapsules formed have dimensions in the range of 50–300 nm for tannic acid.

Matrices with tannic acid–CTAB capsules were obtained at an optimum concentration of 5–9 m*m* tannic acid.

The kinetic studies showed a zero order kinetics process of drug release, the drug amount being controlled by pH of the fluid biological medium.

The zero order kinetics is determined by the processes taking place at molecular level: the chitosan is swelled and the surface is subject to erosion and diffusion, the drug—CTAB capsules are dissolved and will release the active substance (tannic acid) in a zero order kinetic controlled manner diffusion process.

In conclusion, we consider that the tannic acid–CTAB–chitosan matrices are suitable for controlled drug delivery systems.

Acknowledgements This study was financially supported by the CAPACITATI 195 CP-I/2008 and by PN II TD 17/2008 scientific research projects in the frame of the Romanian MEC Programme.

References

1. Maestrelli F, Garcia-Fuentes M, Mura P, Alonso MJ. A new drug nanocarrier consisting of chitosan and hydoxypropylcyclodextrin. Eur J Pharm Biopharm. 2006;63:79–86.
2. Letchford K, Burt H. A review of the formation and classification of amphiphilic block copolymer nanoparticulate structures: micelles, nanospheres, nanocapsules and polymersomes. Eur J Pharm Biopharm. 2007;65:259–69.
3. Moghimi SM, Hedeman H, Muir IS, Illum L, Davis SS. An investigation of the filtration capacity and the fate of large filtered sterically-stabilized microspheres in rat spleen. Biochim Biophys Acta. 1993;1157:233–40.
4. Prego C, Torres D, Fernandez-Megia E, Novoa-Carballal R, Quinoa E, Alonso MJ. Chitosan-PEG nanocapsules as new carriers for oral peptide delivery. J Control Release. 2006;111:299–308.
5. Balau L, Lisa G, Popa MI, Tura V, Melnig V. Physico-chemical properties of chitosan films. Cent Eur J Chem. 2004;2(4):638–47.
6. Trung TS, Thein-Han WW, Qui NT, Ng CH, Stevens WF. Functional characteristics of shrimp chitosan and its membranes as affected by the degree of deacetylation. Bioresour Technol. 2006;97:659–63.
7. Aelenei N, Popa MI, Novac O, Lisa G, Balaita L. Tannic acid incorporation in chitosan-based microparticles and in vitro controlled release. J Mater Sci Mater Med. 2009. doi 10.1007/s10856-008-3675-z.
8. Haslam E. Plant polyphenols: vegetable tannins revisited. Cambridge: Cambridge University Press; 1989.
9. King A, Young G. Characteristics and occurrence of phenolic phytochemicals. J Am Diet Assoc. 1999;99:213–8.
10. Kaul A, Khanduja KL. Polyphenols inhibit promotional phase of tumorigenesis: relevance of superoxide radicals. Nutr Cancer. 1998;32(2):81–5.
11. Kuroda Y, Hara Y. Anitmutagenic and anticarcinogenic activity of tea polyphenols. Mutat Res. 1999;436:69–97.
12. Gali-Muhtasib HU, Yamout SZ, Sidani MM. Tannins protect against skin tumor promotion induced by ultraviolet-B radiation in hairless mice. Nutr Cancer. 2000;37:73–7.
13. Ferguson LR. Role of plant polyphenols in genomic stability. Mutat Res. 2001;475:89–111.
14. Frei B, Higdon JV. Antioxidant activity of tea polyphenols in vivo evidence from animal studies. J Nutr. 2003;133:3275S–84S.
15. Dragsted LO, Strube M, Larsen JC. Cancer-protective factors in fruits and vegetables: biochemical and biological background. Pharmacol Toxicol. 1993;72:116–35.
16. Chung KT, Wong TY, Wei CI, Huang YW, Lin Y. Tannins and human health: a review. Crit Rev Food Sci Nutr. 1998;38:421–64.
17. Weisburger JH. Tea and health: the underlying mechanisms. Proc Soc Exp Biol Med. 1999;220:271–5.
18. Yang CS, Landau JM, Huang MT, Newmark HL. Inhibition of carcinogenesis by dietary polyphenolic compounds. Annu Rev Nutr. 2001;21:381–406.
19. Lambert JD, Yang CS. Mechanisms of cancer prevention by tea constituents. J Nutr. 2003;133:3262S–7S.
20. Chung KT, Wong TY, Wei CI, Huang YW, Lin Y. Tannins and human health: a review. Crit Rev Food Sci Nutr. 1998. doi: 10.1080/10408699891274273.
21. Garlea A, Manole A, Popa MI, Melnig V. Chitosan-paracetamol nanostructure self-assembling matrices as drug delivery systems. Materiale Plastice. 2009;46(4):356–62.
22. Scherrer P. Bestimmung der Größe und der inneren Struktur von Kolloidteilchen mittels Röntgenstrahlen. Göttinger Nachr. 1918;2:98–100.
23. Matsuyama H, Shiraishi H, Kitamura Y. Effect of membrane preparation conditions on solute permeability in chitosan membrane. J Appl Polym Sci. 1999;73:2715–25.
24. Isomaa B, Reuter J, Djupsund BM. The subacute and chronic toxicity of cetyltrimethylammonium bromide (CTAB), a cationic surfaetant, in the rat. Arch Toxicol. 1976;35:91–6.
25. van Ruissen F, Le M, Carroll JM, van der Valk PGM, Schalkwijk J. Differential effects of detergents on keratinocyte gene expression. J Investig Dermatol. 1998;110(4):58–363.
26. Monal WA, Peniche C. Study of the interpolyelectrolyte reaction between chitosan and carboxymethylcellulose. Makromol Chem. 1988;9:693–7.

27. Roberts GAF. Chitin chemistry. London: Macmillan Press; 1992.
28. Focher B, Naggi A, Torri G, Cosanni A, Terbojevich M. Chitosans from *Euphausia superba* 2: characterization of solid state structure. Carbohydr Polym. 1992;18:43–9.
29. Peniche C, Arguelles-Monal W, Davidenko N, Sastre R, Gallardo A, San Roman J. Self-curing membranes of chitosan/PAA IPNs obtained by radical polymerization: preparation, characterization and interpolymer complexation. Biomater. 1999;20:1869–78.
30. Liao S-K, Hung C-C, Lin M-F. A kinetic study of thermal degradations of chitosan/polycaprolactam blends. Macromol Res. 2004;12(5):466–73.